

Fig. 1. Transmission spectrum of NiO from 1μ to 14μ for sample thickness 0.1053 cm , 0.0618 cm , and 0.0386 cm .

double-pass spectrophotometer. Since this finding pointed towards some interesting information concerning the semiconducting properties of NiO, a more careful study was begun. Because refractive index information is necessary to convert transmission to absorption coefficient, and few refractive index data are available,⁴ the following technique was adopted to obtain both refractive index and absorption coefficient data from the transmission spectrum.

The transmission T of a plane parallel plate of thickness x can be expressed by the equation⁵

$$T = \frac{(1-R)^2 e^{-\alpha x}}{1 - R^2 e^{-2\alpha x}}, \quad (1)$$

where α is the absorption coefficient and R is the reflection coefficient defined as $R = [(n-1)/(n+1)]^2$, with n as the refractive

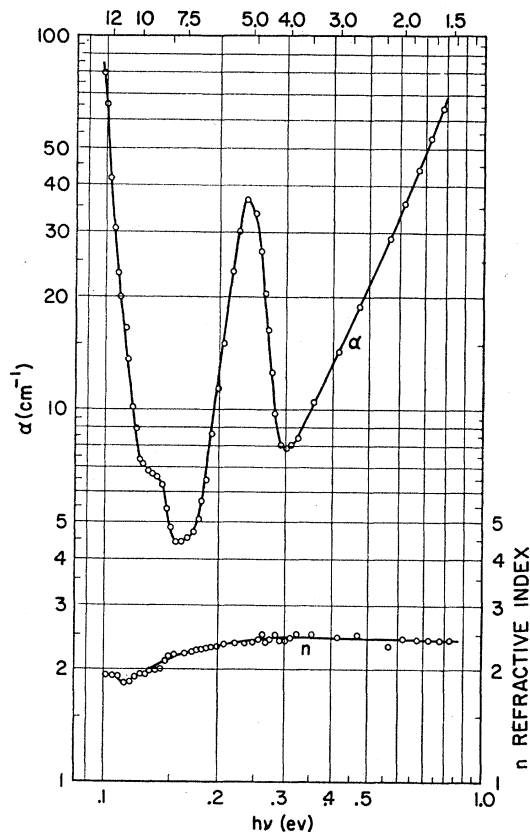


Fig. 2. Absorption coefficient α (cm^{-1}) and refractive index n of NiO versus photon energy in eV.

index. The n and α values could be derived from an algebraic simultaneous solution of the equations for two different thicknesses; however, in this case, a graphical solution was used which combined the data on specimens of three different thicknesses. The graphical solution was obtained by plotting from Eq. (1), T versus αx with $n(R)$ as a parameter. Trial values of n then permitted the determination of α for known x and n ; α and n values which were independent of thickness x were thereby chosen.

The $1 \times 5 \times 10\text{ mm}$ cleaved plate was ground and polished optically flat and parallel and the transmission spectrum obtained. This same plate was then ground and repolished for two thinner specimens. The transmission spectra (Fig. 1) for the three thicknesses (0.1053 cm ; 0.0618 cm ; 0.0386 cm) are replotted as absorption coefficient versus photon energy in Fig. 2, utilizing the graphical solution outlined above. Refractive index data obtained from the solution are also included and agree fairly well with those published.⁴

The branch of the curve for energy values greater than 0.3 eV may be the tail of the fundamental absorption which is to be expected at about 2 eV according to the electrical measurements of Wright and Andrews⁶ on polycrystalline NiO. These authors present data indicating the existence of impurity optical activation energies between 0.3 and 0.6 eV . The 0.24-eV absorption peak may be an impurity ionization energy corresponding at least in order of magnitude to that expected above. There is also a satellite absorption peak at 0.13 eV . The increasing absorption coefficient below this peak is probably a lattice vibration absorption. The validity of this conclusion is enhanced by the suddenly decreasing refractive index at these low frequencies, a circumstance which probably would not result from impurity absorption.

We would like to thank Dr. G. G. Palmer, who supplied us with the NiO crystals, and Dr. F. G. Keihn, who made the x-ray determinations on them for us.

¹ A. Verneuil, Compt. rend. 135, 791 (1902); Ann. chim. et phys. 3, 20 (1904).

² H. P. Rooksby, Nature 152, 304 (1943).

³ E. J. W. Verwey, in *Semiconducting Materials* (Butterworths Scientific Publications Ltd., London, 1951), p. 155.

⁴ C. J. Ksanda, Am. J. Sci. 22, 131 (1931); A. Kundt, Sitzber. deut. Akad. Wiss. Berlin, 255-272 (1888).

⁵ R. B. Barnes and M. Czerny, Phys. Rev. 38, 338 (1931).

⁶ R. W. Wright and J. P. Andrews, Proc. Phys. Soc. (London) 62, 446 (1949).

Bulk Photoconductivity in Lead Sulfide*

D. E. SOULE AND R. J. CASHMAN
Department of Physics, Northwestern University, Evanston, Illinois
(Received December 7, 1953)

EXTENSIVE investigations have been carried out upon photoconducting evaporated and chemical layers of PbS (for a review see Smith¹). Sosnowski *et al.*² and Gibson³ have presented models of photoconductivity in evaporated layers based on the modulation of intercrystalline potential barriers. Experimental evidence of bulk photoconductivity in PbS crystals, however, has not been published to our knowledge. We have studied this property in three cleaved synthetic PbS crystals at liquid nitrogen temperature.

The dark conductivities at room temperature for samples S_{11} , S_{12} , S_{13} were 34 , 21 , and $23\text{ ohm}^{-1}\text{ cm}^{-1}$, respectively. All electrode and probe contacts to the crystals were made by electroplating them with rhodium and then soldering the lead wires to the rhodium. All samples showed slight internal rectification.

The potential difference developed between a probe fixed at the right electrode and a probe moved along the crystal S_{12} at room temperature is shown in Fig. 1(a). Two different traversing paths are represented. Potential barriers are present within the crystal at A , B , C , and D .

At 77°K the frequency response to chopped radiation from a tungsten source was taken over the range of 20 to 9000 cps to

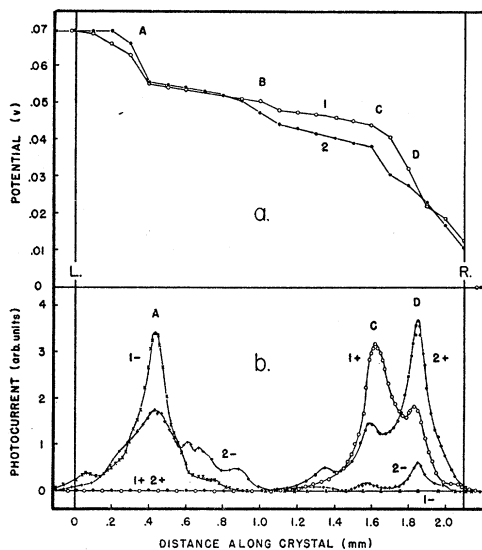


FIG. 1. (a) Potential versus distance along crystal at room temperature. 1 and 2 are different paths. (b) Photocurrent response at 77°K for light spot (width 75 μ) scanned along crystal. Paths 1 and 2 correspond roughly to those in (a). Sign indicated is for the right electrode.

determine the possibility of a thermal contribution to the resultant current change. During the measurement the electrode-to-crystal junctions were masked. Throughout this frequency range the photoresponse remained constant to within ± 2.0 percent. An upper limit of 4 microseconds for the time constant was calculated assuming a maximum of 2.0 percent drop in amplitude at 9000 cps from that at 20 cps. All following photocurrent measurements were made with a tungsten source chopped at 90 cps with the crystal at 77°K.

The surface was then scanned with a light spot 75 μ wide. A 0.54 v bias was applied in the back direction (right electrode positive) and 0.50 v in the forward direction. The resulting photocurrent is shown in Fig. 1(b) for both polarities of applied voltage and for two different traversing paths along S_{12} corresponding roughly to those followed in Fig. 1(a). No appreciable photoresponse appears to originate at the metal to semiconductor junctions of the electrodes at L and R. The photoresponse maxima located at A, C, and D correspond to the potential barriers at A, C, and D, respectively, in Fig. 1(a). For both paths where the right electrode is positive the left-hand maxima are depressed and vice versa. This behavior indicates that the barriers are asymmetrical and are modulated by the applied voltage. Thermoelectric probe measurements taken over the whole crystal surface showed it to be p type. Consequently, the carrier concentration across a barrier is probably a gradation in hole density.

The photocurrent dependence upon applied bias voltage with the total crystal illuminated showed maximum responses at 0.9 v for the right electrode positive and 0.7 v for the right electrode negative. The reason for this apparent saturation effect is not yet known.

It appears evident from these measurements that though these internal potential barriers may not necessarily be the original sites of the primary photoeffect they at least aid in rendering the photocurrent measurable.

This investigation is still in progress and a more complete report will be published at a later date.

* This work was sponsored by the U. S. Bureau of Ships, Department of the Navy, Washington, D. C.

¹ R. A. Smith, *Advance in Physics* 2, 321 (1953).

² Sosnowski, Starkiewicz, and Simpson, *Nature* 159, 818 (1947).

³ A. F. Gibson, *Proc. Phys. Soc. (London)* B64, 603 (1951).

Generalized Fermi-Thomas Theory

MALCOLM K. BRACHMAN

Texas Instruments Incorporated, Dallas, Texas

(Received October 23, 1953; revised manuscript received December 11, 1953)

THE virial theorem for the generalized Fermi-Thomas theory of Feynman, Metropolis, and Teller¹ has been further discussed by the author² and by March.³ It is possible to avoid the long sequence of operations used in the analytical proof of reference 1 by employing a single integration by parts of the expression for E_{kin} combined with Duffin's lemma,⁴ the known relation

$$\partial I_\nu(\eta)/\partial\eta = \nu I_{\nu-1}(\eta)$$

and the known value of the pressure.²

Reference 2 treats a system of Z electrons moving in the field of a nucleus of charge Ze and infinite mass. The electrons interact with one another according to Coulomb's law and obey the Fermi-Dirac statistics. If we set the electronic charge e equal to zero so that the Coulomb interaction is omitted, we obtain the thermodynamic functions recently given by Singwi⁵ for a system of particles obeying the Pauli exclusion principle but without further interactions; this corresponds to the model of liquid He³ envisaged in reference 5. To complete the identification, we note that $R = Zk$ and $\rho = Z/v$. A general expression for the pressure is

$$p = \frac{2}{3} \frac{I_1(\eta)}{I_1(\eta)} \frac{RT}{v},$$

which reduces to the correct value $\frac{2}{3}\rho\epsilon_0$ when T tends to zero.

- ¹ Feynman, Metropolis, and Teller, *Phys. Rev.* 75, 1561 (1949).
² M. K. Brachman, *Phys. Rev.* 84, 1263 (1951).
³ N. H. March, *Phil. Mag.* 43, 1042 (1952); 44, 346 (1953).
⁴ R. J. Duffin, *Phys. Rev.* 47, 421 (1935).
⁵ K. S. Singwi, *Phys. Rev.* 87, 540 (1952).

The Spread of the Soft Component of Cosmic Radiation

G. MOLIERE

Centro Brasileiro de Pesquisas Físicas, Rio de Janeiro, Brazil

(Received December 8, 1953)

IN a paper under the same title,¹ Green and Messel criticized "all previous work" on the subject in question. A reply to their criticism seems worth while in order to avoid confusion and to clarify the situation.

(1) Green and Messel's criticism concerns first the higher angular and radial moments, due to multiple Coulomb scattering, of the cascade electrons of a given energy. The numerical values of these higher moments depend essentially on the manner in which the effect of single scattering is taken into account. With respect to this, the following cases can be distinguished.

A. *Pure multiple scattering*:—this is the approximation of Landau's equations. Single scattering is entirely neglected and the angular and radial distribution functions $f(E, \theta)$ and $f(E, r)$, therefore, fall off too rapidly at large values of the arguments θ and r . The higher moments are closely connected with the fall-off at large values of the arguments and are, therefore, strictly speaking, without physical significance in this approximation. Nevertheless, their computation can be useful. These are the higher moments which have been calculated exactly by Eyges and Fernbach.² In the present author's theory³ these higher moments were duly taken into account up to a certain stage of the calculation (see Sec. B).

B. *Single scattering is taken into account with due consideration of the effect of the finite size of the nuclei*:—this is, in principle, the most exact procedure and it is this which was proposed by Green and Messel in their paper. The limitation of the large single scattering angles as a consequence of the finite size of the nucleus, may be taken into account (according to E. J. Williams)